Int. J. Electrochem. Sci., 16 **(2021)** Article Number: 211223, doi: 10.20964/2021.12.37

International Journal of
ELECTROCHEMICAL
SCIENCE
www.electrochemsci.org

Short Communication

Fabrication of a Co_3O_4/ZnO Heterostructure by Electrochemical Deposition

Masaya Ichimura[*], *Yuzuki Tomita*

Department of Electrical and Mechanical Engineering, Nagoya Institute of Technology, Nagoya 466-8555, Japan
[*]E-mail: ichimura.masaya@nitech.ac.jp

Received: 30 August 2021 / *Accepted:* 1 October 2021 / *Published:* 10 November 2021

Co_3O_4 thin films were fabricated using electrochemical deposition (ECD). $Co(OH)_2$ precursor films were deposited galvanostatically from an aqueous solution containing $Co(NO_3)_2$ and NH_4NO_3, and subsequently converted to Co_3O_4 by annealing in the air ambient. The Co_3O_4 films had two absorption edges corresponding to energy levels of 1.5 and 2.0 eV, and exhibited a clear p-type photo response in the photoelectrochemical measurement. The pn heterostructures were fabricated with ZnO as the n-type partner. ZnO was first deposited using ECD, $Co(OH)_2$ was subsequently deposited on it, and finally the sample was annealed. The fabricated Co_3O_4/ZnO structure exhibited clear rectification properties.

Keywords: electrochemical deposition, Co_3O_4, ZnO, heterostructure, diode

1. INTRODUCTION

Whereas impurity doping in Si and III-V semiconductors can satisfactorily control the conduction, the valence control by doping is difficult for many oxide semiconductors. Thus, separate n- and p-type materials are used to construct a pn heterojunction in the oxide electronics technology. Many metal oxides, such as ZnO, SnO_2, TiO_2, and Fe_2O_3, are available as n-type materials. A p-type material is needed to construct a pn heterojunction; however, only a few p-type materials exist among metal oxides. Cu_2O has been widely studied as the most popular p-type metal oxide to fabricate Cu_2O-based heterostructures. In addition, Co_3O_4 is an inherently p-type semiconductor with a bandgap of approximately 1.5 eV. Co is an abundant and inexpensive element, which is available on the earth's crust at the same order of magnitude as Cu and Zn. Although Co_3O_4 is a typical catalyst, the fabrication of Co_3O_4-based pn junction has been scarcely investigated. Co_3O_4/TiO_2 solar cells were fabricated by Kupfer et al. using spray pyrolysis of TiO_2 and pulsed laser deposition of Co_3O_4 [1]. Lohaus et al.

reported the fabrication of $NiO/Co_3O_4/TiO_2$ cells using the RF-magnetron sputtering [2], where the cell did not exhibit rectification without TiO_2 or NiO. Patel et al. achieved a high efficiency of 0.6% for $NiO/Co_3O_4/TiO_2$ cells with Ag-nano-wire contact, where Co_3O_4 layers were grown using DC sputtering [3]. Additionally, they also fabricated Co_3O_4/ZnO photovoltaic cells [4]. Ghamgosar et al. used DC sputtering to deposit Co_3O_4 and fabricate Co_3O_4/ZnO-nano-wire photodetectors [5].

In this study, we fabricated Co_3O_4-based pn diodes using electrochemical deposition (ECD). ECD is a simple, low-cost technique, and capable of large area deposition, which has been widely examined for cobalt oxide [6–15]. Films deposited at room temperature are considered to be $Co(OH)_2$ or CoOOH, which are useful as a catalyst. $Co(OH)_2$ deposited using ECD can be converted to Co_3O_4 by annealing at temperatures above 200°C [11–15]. Although cobalt oxide and hydroxide obtained using ECD have been extensively applied in catalysts and electrodes, their semiconducting properties have not been adequately investigated. Ebadi et al. and Ma et al. used ECD-Co_3O_4 as a photocathode for hydrogen generation, where Co_3O_4 acted as a photoconductive p-type semiconductor [14,15]. To the best of our knowledge, ECD-Co_3O_4 has never been applied in semiconductor devices, including a pn junction.

p-type Co_3O_4 should be combined with an n-type material to fabricate a heterostructure diode. We selected ZnO as a partner of heterostructure for which ECD is completely developed. In addition to the studies on photovoltaic devices based on Co_3O_4/ZnO, other studies have investigated Co_3O_4/ZnO electrochemical electrodes in which Co_3O_4 acts as a catalyst for ZnO electrodes [16,17], and Co_3O_4/ZnO photocatalysts in which Co_3O_4 enhances the separation of photogenerated electrons/holes [18–20].

The rest of this paper is organized as follows. In Section 2, the deposition condition of the respective layer is described. Section 3 presents the properties of Co_3O_4 films in detail, and discusses diode properties of the proposed heterostructure. Section 4 draws the conclusions.

2. EXPERIMENTAL

ECD was carried out galvanostatically using the potentiostat/galvanostat; model: HA151-B (Hokuto Denko). The substrate (operating electrode) and counter electrode were indium-tin-oxide (ITO) coated glass sheet and Pt sheet, respectively. The deposition solution for cobalt oxide was an aqueous solution containing 20 mM of $Co(NO_3)_2$ and 100 mM of NH_4NO_3 [15]. The deposition temperature, current, time, and area were 60°C, 5 mA/cm^2, 1 min, and 1 cm × 1 cm, respectively. The deposition solution for ZnO contained 100 mM of $Zn(NO_3)_2$, whereas the deposition temperature, current, and time were 60°C, 1.5 mA/cm^2, and 10 min, respectively.

Additionally, annealing was performed at temperatures in the range of 100°C–400°C in the ambient air to convert as-deposited $Co(OH)_2$ to Co_3O_4. In the heterostructure fabrication, ZnO was deposited first, followed by $Co(OH)_2$ deposited on it. Subsequently, the heterostructure sample was annealed at 400°C.

The film thickness was evaluated using the surface profiler Surfcom 1400D (Tokyo Seimitsu). Composition was measured using an Auger electron spectroscopy (AES) microprobe; model: JEOL JAMP- 9500F. Ar sputtering was performed to clean the surface before the AES measurement. Moreover, the same instrument was used for scanning electron microscopy (SEM). Optical absorption

was measured using a spectrophotometer JASCO V-570. A Raman spectroscope (JASCO NRS-3300) was used to observe Raman scattering; the excitation laser wavelength was 532 nm. Photo-responsivity and conduction type of the films were characterized using the photoelectrochemical (PEC) measurement. A standard three-electrode electrochemical cell was used with an Ag/AgCl reference electrode. The sample was immersed in 100 mM of Na_2SO_4 aqueous solution. The potential was scanned at a scan rate of 5 mV/s, whereas the sample was irradiated with the light of solar simulator Abet 10 500 (100 mW/cm^2) intermittently at an interval of 5 s. For electrical characterization, In electrodes (1 mm × 1 mm) were fabricated using vacuum evaporation. The solar simulator was used to measure the photo response of the devices.

3. RESULTS AND DISCUSSION

The as-deposited film had a blue-white color, and its thickness was a 0.75 μm for a 1 min deposition. After annealing at temperatures above 200°C, the film color turned to black. Figure 1 shows optical transmittance of the as-deposited and annealed films.

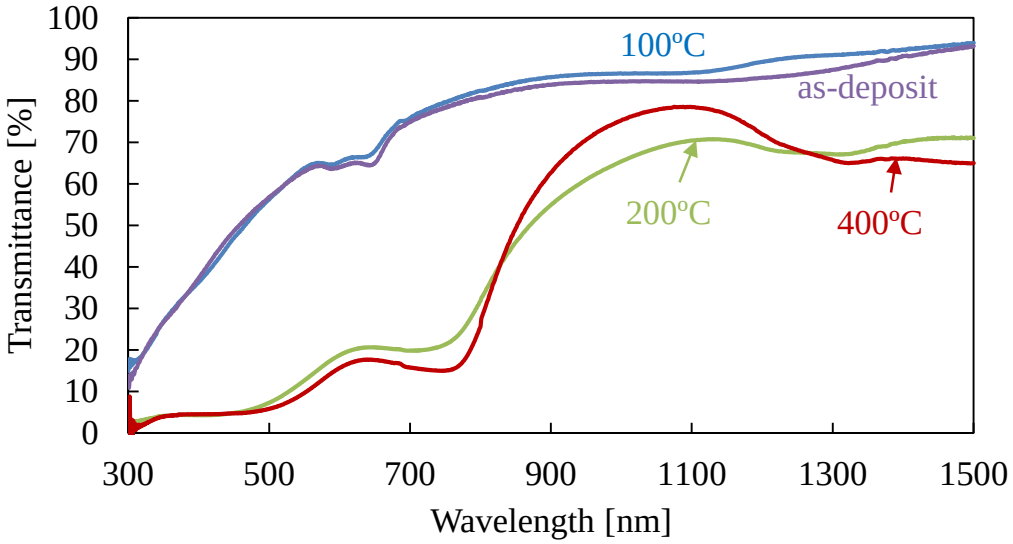

Figure 1. Optical transmission spectra of the as-deposited $Co(OH)_2$ films and the annealed films.

The as-deposited and annealed films at 100°C have an absorption edge of approximately 500 nm, and the transmission in the visible range is approximately 80%. For the two samples, the observed absorption was expected to correspond to the inter-band transition of $Co(OH)_2$ [21]. The annealed films at 200°C and 400°C seem to have two absorption edges near 800 and 600 nm. Therefore, the phase change from $Co(OH)_2$ to Co_3O_4 occurs by annealing at temperatures above 200°C. Some existing studies have presented comparable annealing behaviors [11–15]. Two bandgaps are commonly observed for Co_3O_4: the first absorption edge for the annealed films at 200°C and 400°C was near 800 nm, which is

attributed to the transition between Co^{3+} and O^{2-} (or the valence band), and the second one is attributed to the transition between Co^{2+} (or the conduction band) and O^{2-} [21–23]. According to the Tauc plot, the first and second absorption edges correspond to the bandgap energies of 1.5 and 2.0 eV, respectively, which satisfactorily agree with the results obtained in some of the existing studies [21–23].

Figure 2 shows the Raman spectra for the as-deposited and annealed films. For the as-deposited and annealed films at 100°C, we did not observe any peaks associated with $Co(OH)_2$ or Co_3O_4. The peaks marked with the triangles are owing to the presence of ITO, and the peak near 905 cm^{-1} was not identified. After annealing at temperatures above 200°C, the peaks caused by Co_3O_4 were observed [24]. Thus, the Raman results indicate the conversion of $Co(OH)_2$ to Co_3O_4 at temperatures above 200°C.

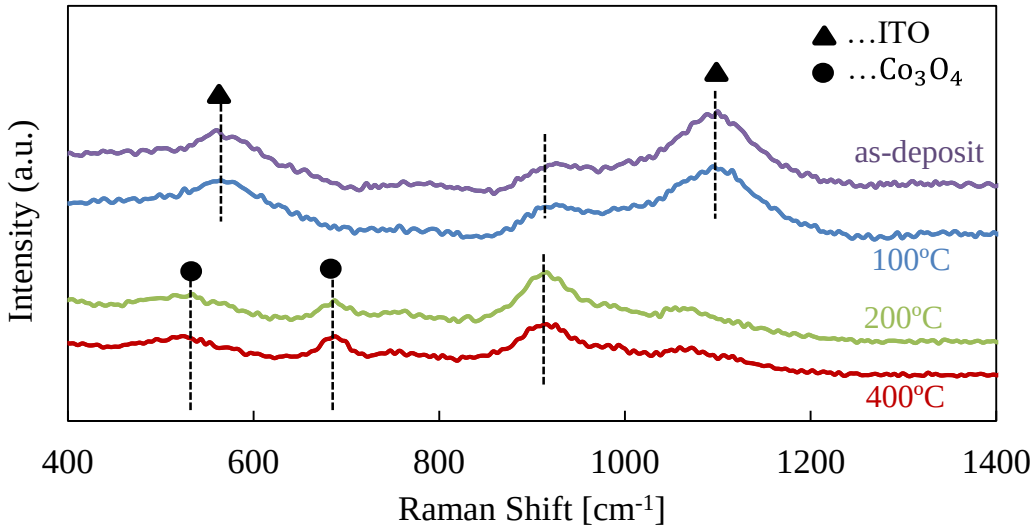

Figure 2. Raman spectra of the as-deposited $Co(OH)_2$ films and the annealed films.

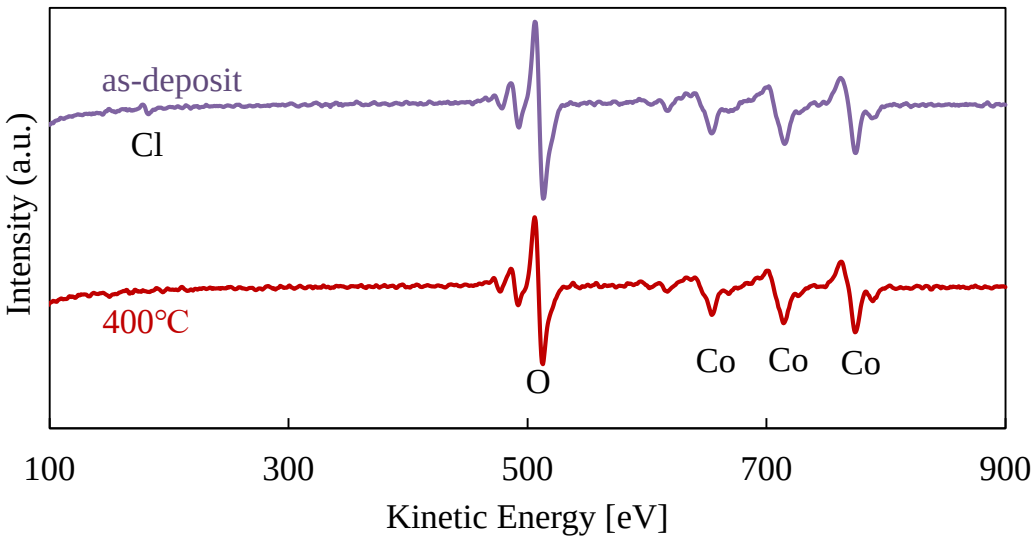

Figure 3. AES spectra of the as-deposited $Co(OH)_2$ films and the 400ºC annealed films.

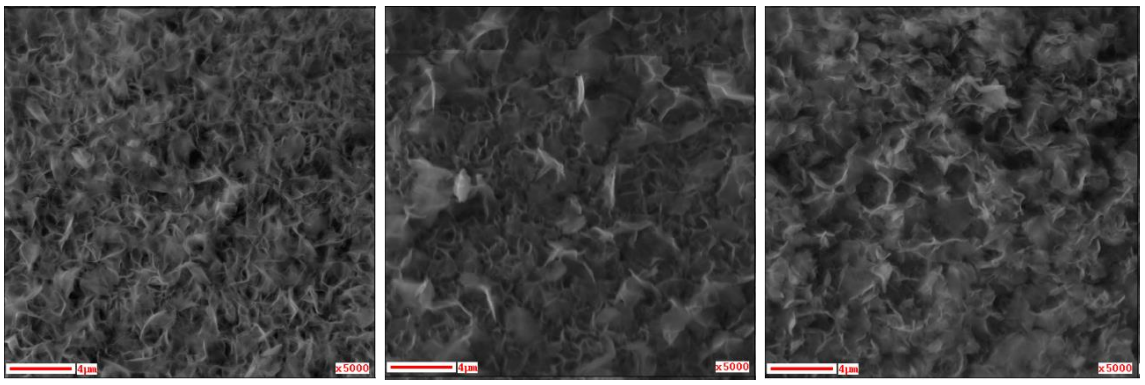

Figure 4. SEM images of (a) the as-deposited film, (b) the film annealed at 100 ºC, and (c) the film annealed at 400 ºC.

Figure 3 shows the AES spectra for the as-deposited and annealed films at 400°C wherein the film consists of Co and O. The elemental composition ratios were calculated using the AES data, whereas commercially available data for Co_3O_4 were used as the reference. The O/Co ratio is 1.5 and 1.3 for the as-deposited and annealed (400°C) films, respectively. Hence, the latter is close to the stoichiometric ratio (4/3) for Co_3O_4, and the ration decrease by annealing is attributed to the conversion of $Co(OH)_2$ to Co_3O_4. However, the ratio for the as-deposited film is smaller than the stoichiometric ratio (2) for $Co(OH)_2$. This is because the hydroxide is partly decomposed by the Ar sputtering before the AES measurement.

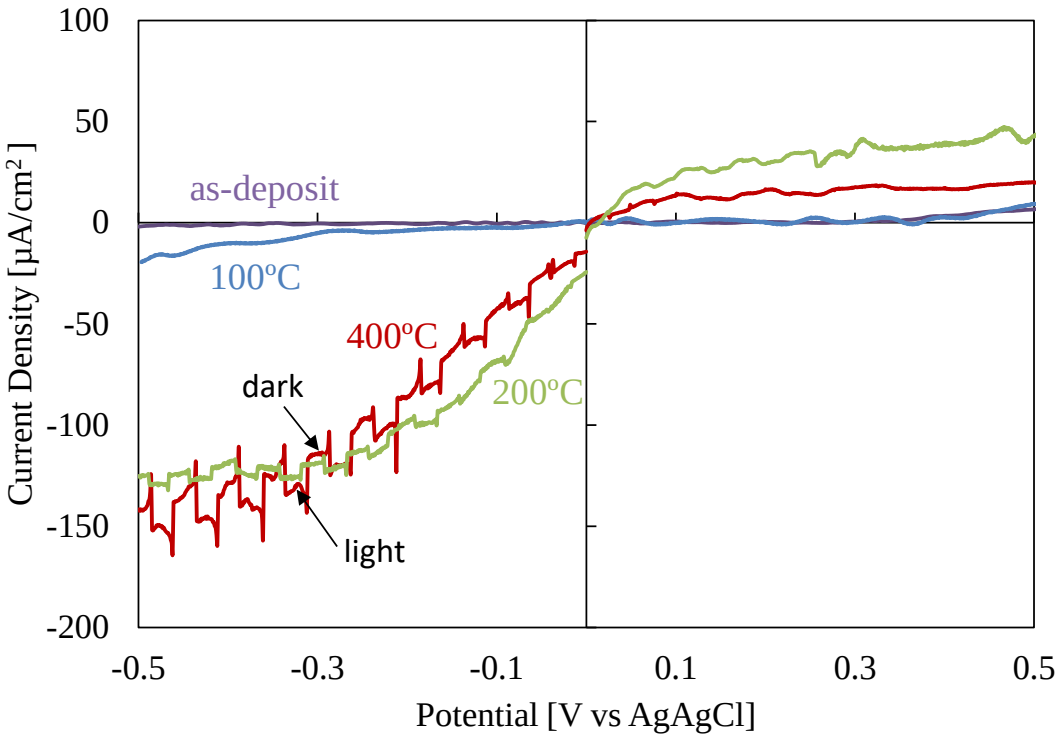

Figure 5. Photoelectrochemical results of the as-deposited $Co(OH)_2$ films and the annealed films.

The SEM images of the as-deposited and annealed films are shown in Figure 4. The observed sheet-like structure of the as-deposited film, which grows perpendicular to the substrate, agrees with that presented by Ma et al. [15]. The structure seems to be preserved even after annealing.

The PEC results for the as-deposited and annealed films are shown in Figure 5. In the PEC measurement, photo response owing to minority carriers is observed dominantly. Significant photo response cannot be observed for the as-deposited and annealed (100°C) films either in the positive or negative bias range, indicating that the $Co(OH)_2$ film does not exhibit photoconductivity. A negative photo current was observed in the negative bias range for the annealed (200°C and 400°C) samples. The negative PEC response implies that the minority carrier is electron; thus, the conduction is of p-type. Thus, after the conversion to Co_3O_4 by annealing, the samples behave as a p-type semiconductor. The photo current of the film annealed at 400°C was larger than that of the film annealed at 200°C. Therefore, in the heterostructure fabrication, the samples were annealed at 400°C.

The Co_3O_4/ZnO heterostructure was fabricated by the ECD of ZnO, ECD of $Co(OH)_2$, and subsequent annealing at 400°C. Thickness of ZnO was in the range of 1.0–1.5 µm. Figure 5 shows the current-voltage (I-V) characteristics of the Co_3O_4/ZnO heterostructure diode in the dark and under an AM1.5 illumination. A clear rectification can be observed, and photoconductivity is confirmed; thus, the current increases under the illumination; however, photovoltaic effects cannot be confirmed.

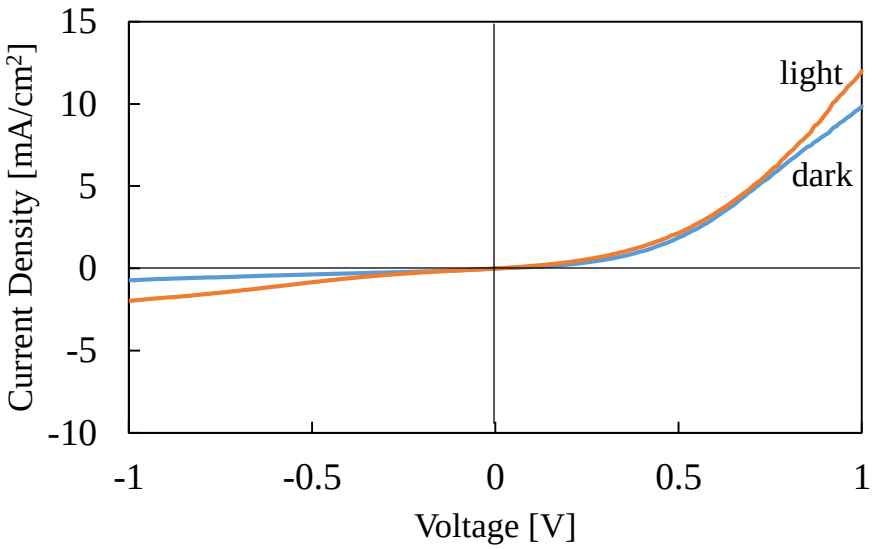

Figure 6. I-V characteristics in the dark and under AM1.5 illumination for the Co_3O_4/ZnO heterostructure device.

As noted in the introduction, two groups have reported Co_3O_4/ZnO heterostructure devices. Patel et al. fabricated a MoO_3/Co_3O_4/ZnO photovoltaic cell. They found that the output was considerably smaller without the MoO_3-hole-transport layer [4]. The fill factor of the solar cell was 0.25 with or without MoO_3, and thus the I-V characteristics (rectification properties) were moderately poor. Ghamgosar et al. fabricated Co_3O_4/ZnO-nano-wire devices with an inserted Al_2O_3 interface layer [5].

The photovoltaic output was extremely low without Al_2O_3, and I-V characteristics exhibited a weak rectification even with Al_2O_3. They used Au as the electrode, which could act as a Schottky contact for ZnO. Thus, their device was expected to exhibit rectification and photovoltaic effects even without Co_3O_4. The best performance was achieved for a device with an extremely thin (thickness = 1 nm) Co_3O_4 layer, whereas an increase in the thickness of Co_3O_4 deteriorated the obtained characteristics. Thus, I-V characteristics of Co_3O_4/ZnO heterostructure devices have been typically poor, and the performance can be improved using a hole-transport over-layer (equivalently a Schottky metal) or a wide bandgap interfacial layer. An effective improvement by the hole-transport layer indicates that the band bending at the Co_3O_4/ZnO interface is not sufficiently large for a clear rectification as the work function difference between Co_3O_4 and ZnO is not large enough. An over-layer with a work function larger than Co_3O_4 can enhance the total work function difference and band bending. Therefore, the band alignment at the Co_3O_4/ZnO interface should be determined for further exploration; however, it has not been investigated yet. Moreover, an improvement in the diode characteristics using the interfacial layer indicates a large density of defect states at the Co_3O_4/ZnO interface. An irregular bonding at the interface (Co–O–Zn) may induce gap states. The defects at the interface can act as a leakage path and deteriorate the diode characteristics. Such a leakage can be diminished using an interfacial layer with a large bandgap. In addition, in ECD fabrication of a heterostructure, the underlying first layer could be partly dissolved in the deposition solution of the second layer because of the lack of chemical equilibrium between the first layer and the solution. Consequently, the heterointerface cannot have an abrupt composition profile; however, it can have a transition region with a gradual composition change. This can also deteriorate the pn junction properties. Because the Co_3O_4 layer of our device is not extremely thin, deposition of an over-layer cannot effectively modify the band bending at the Co_3O_4/ZnO interface. In the future study, we will attempt to introduce a chemically stable interfacial layer, such as Al_2O_3, to improve the diode properties, suppress the formation of the transition layer, and reduce the leakage current.

4. SUMMARY

We fabricated Co_3O_4 thin films using the ECD of $Co(OH)_2$ precursor and subsequent annealing in the air ambient. The Co_3O_4 films had two absorption edges corresponding to the energy levels of 1.5 and 2.0 eV, and exhibited a clear p-type photo response in the PEC measurement. The pn heterostructures were fabricated with the ECD-ZnO as the partner of heterojunction. In addition, the C_3O_4/ZnO structure exhibited rectification properties. To the best of our knowledge, the ECD fabrication of Co_3O_4-based heterostructure devices were first introduced in this study.

References

1. B. Kupfer, K. Majhi, D.A. Keller, Y. Bouhadana, S. Rühle, H.N. Barad, A.Y. Anderson and A. Zaban, *Adv. Energy Mater*., 5 (2015) 1401007.
2. C. Lohaus, J. Morasch, J. Brotz, A. Klein and W. Jaegermann, *J. Phys. D Appl. Phys*., 49 (2016)

155306.
3. M. Patel, S.H. Park and J. Kim, *Phys. Status Solidi,* A 215 (2018) 1800216.
4. M. Patela, M. Kumar, H.S. Kima, W.H. Park, E.H. Choic and J. Kim, *Mater. Sci. Semicond. Proc.,*74 (2018) 74.
5. P. Ghamgosar, F. Rigoni, M.G. Kohan, S.You, E.A. Morales, R. Mazzaro, V. Morandi, N. Almqvist, I. Concina and A. Vomiero, *ACS Appl. Mater. Interfaces,* 11 (2019) 23454.
6. P.M.S. Monk, S.L. Chester, D.S. Highman and R.D. Partridge, *Electrochim. Acta,* 39 (1994) 2271.
7. E.B. Castro, C.A. Gervasi and J.R. Vilche, *J. Appl. Electrochem*., 28 (1998) 835.
8. K. Nakaoka, M. Nakayama and K.Ogura, *J. Electrochem. Soc*., 149 (2002) C159.
9. T. Pauporte´, L. Mendoza, M. Cassir, M.C. Bernard and J. Chivot, *J. Electrochem. Soc*., 152 (2005) C49.
10. J.R.S. Brownsona and C. Lévy-Clément, *Electrochimica Acta,* 54 (2009) 6637.
11. Y.C. Liu, J.A. Koza and J.A. Switzer, *Electrochimica Acta,* 140 (2014) 359.
12. S.G. Kandalkar, H.M. Lee, H. Chae and C.K. Kim, *Mater. Res. Bull*., 46 (2011) 48.
13. P.T. Babara, A.C. Lokhandea, B.S. Pawarb, M.G. Ganga, Eunjin Joa, C. Goa, M.P. Suryawanshia, S.M. Pawarb and J.H. Kim, *Appl. Surf. Sci.,* 427 (2018) 253.
14. M. Ebadi, M.A. Mat-Teridi, M.Y. Sulaiman, W.J. Basirun, N. Asim, N.A. Ludin, M.A. Ibrahim and K. Sopian, *RSC Adv*., 5 (2015) 36820.
15. Y. Mao, W. Li, P. Liu, J. Chen and E. Liang, *Mater. Lett*., 134 (2014) 276.
16. N. Koteeswara Reddy, S. Winkler, N. Koch and N. Pinna, *ACS Appl. Mater. Interfaces,* 8 (2016) 3226.
17. H. Wu, S. Li, X. Lu, C.Y. Toe, H.Y. Chung, Y. Tang, X. Lu, R. Amal, L. Li and Y. H. Ng, *Chem Plus Chem.,* 83 (2018) 934.
18. N. Liua and Z. Li, *Mater. Sci. Semicond. Proc*., 79 (2018) 24.
19. C. Dong, X. Xiao, G. Chen, H. Guan and Y. Wang, *Mater. Chem. Phys*., 155 (2015) 1.
20. Y. Yang, W. Cheng and Y.F. Cheng, *Appl. Surf. Sci*., 476 (2019) 815.
21. M. Martínez-Gil, D. Cabrera-German, M.I. Pintor-Monroy, J.A. García-Valenzuela, M. Cota-Leal, W. De la Cruz, M.A. Quevedo-Lopez, R. Perez-Salas and M. Sotelo-Lerma, *Mater. Sci. Semicond. Proc.,* 107 (2020) 104825.
22. C.S. Cheng, M. Serizawa, H. Sakata and T. Hirayama, *Mater. Chem. Phys*., 53 (1998) 225.
23. D. Barreca, C. Massignan, S. Daolio, M. Fabrizio, C. Piccirillo, L. Armelao and E. Tondello, *Chem. Mater*., 13 (2001) 588.
24. Y.C. Liu, V.G. Hadzhiev, M.N. Iliev and I.V. Vergilov, *J. Phys. C. Solid State Phys*., 21 (1988) L199.